Condensed Matter Physics 2008, Vol. 11, No 1(53), pp. 95–106

CONDENSED MATTER PHYSICS

Multiple time scales in the microscopic dynamics of simple and complex liquids as studied by radiation scattering

F.J.Bermejo[1]*, F.Fernandez-Alonso[2,3], C.Cabrillo[1]

[1] Instituto de Estructura de la Materia, C.S.I.C. and Unidad Asociada de Investigación en Física Aplicable, Dept. Electricidad y Electónica, Facultad de Ciencia y Tecnología, Universidad del País Vasco/ Euskal Herriko Unibertsitatea, P.O.Box 644, E–48080 Bilbao, Spain

[2] ISIS Facility, Rutherford Appleton Laboratory, Chilton, Didcot, Oxfordshire OX11 0QX, United Kingdom

[3] Department of Physics and Astronomy, University College London, Gower Street, London WC1E 6BT, United Kingdom

Received October 10, 2007

Experimental investigations into the time-scales spanned by the microscopic dynamics of simple (metallic) and molecular liquids, as explored by neutron scattering and muon spin rotation experiments are reviewed.

Key words: *dynamics, liquids, glasses, neutron scattering, muon spectroscopy*

PACS: *61.25.Mv, 66.10.-x, 66.30.Fq, 65.20.+v*

1. General overview

Our knowledge of the microscopic details governing atomic and molecular motions in liquids goes back to the mid 19th century when Stokes [1] considered the motion of a macroscopic spherical particle of radius a immersed in a continuum of viscosity η. The translational motion of such a sphere, which was assumed to move with uniform velocity and no slippage of the fluid layer adjacent to it, was found to be the result of two forces acting on it, namely, $f_1 = 4\pi a\eta$ resulting from pressure built in the front of the moving particle and a frictional component $f_2 = 2\pi a\eta$ parallel to the particle surface. The resulting friction term yields $\xi = 6\pi a\eta$. Later, Einstein [1] showed that the mass self-diffusion coefficient for the moving particle is related to such friction term by $D_{\rm T} = k_{\rm B}T/\xi$. The beauty of Einstein's approach was that it enabled direct comparison with experiment. The underlying probability density associated with the stochastic process governing the time-dependent position of the Brownian particle also solves Fick's diffusion equation and yields a quantitative measure for the mean-square distance $\langle u^2\rangle$ that a particle moves in a time t, $\langle u^2\rangle = 6D_{\rm T}t$.

The Stokes-Einstein (SE) approach is severely simplified since the momentum of the moving particle is ignored. This leads to an unphysical result for the average velocity of the particle $v = \sqrt{3D_{\rm T}/2t}$ with the obvious consequence of a divergent behavior at short times. As first suggested by Smoluchowski, the paradox is solved if the particle drift velocity is allowed to depend on its position, and an approach based upon the Langevin picture is adopted. If the particle feels the action of a field like gravity, an equivalent expression for the SE relation is replaced by the Nernst-Einstein (NE) equation $D_T = k_{\rm B}T/\xi_{\rm NE}$ where $\xi_{\rm NE}$ is now a friction coefficient $\xi_{\rm NE} = \vec{F}/\vec{v}$ that is now related to the force and terminal velocity of the diffusing particle. The prediction now made is that at short times the particle velocity should become $\sqrt{3k_{\rm B}T/2M}$ where M stands for the particle mass, which removes the inconsistency mentioned above, and also tells us that at times longer than the relaxation time for the average momentum $\tau_Q = M/\xi_{\rm NE}$, the expression for $\langle u^2\rangle$

*E-mail: javier@langran.iem.csic.es

equates that given above. Particle diffusion thus becomes a well-defined quantity for times longer than τ_Q and its characteristic times are given in terms of $\tau_{\rm diff} \propto 1/D_{\rm T}$.

On fully analogous grounds, Debye [2] considered the rotation of a spherical molecule in a continuum. Within the Stokes approach, this molecule is subjected to a rotational friction coefficient $\xi_{\rm R} = 8\pi a^3\eta$. The reorientational motion of such object obeys a rotational diffusion equation, usually referred to as the Stokes-Einstein-Debye (SED) relationship, with coefficient $D_{\rm R} \propto 1/\tau_{\rm R}$ which, in turn, defines a characteristic timescale for molecular rotations.

Both the SE and SED methods encounter a number of difficulties if applied by brute force to neat liquids. The first difficulty is to specify the size of a moving molecule. In fact, unphysically small volumes are usually needed to fit experimental data. Second, for a liquid of like molecules, the size of the molecules surrounding the tagged particle does matter, and a number of approaches have been suggested to deal with this added complication [3]. Finally, the data available so far indicate that while the translational diffusion coefficient senses quite sensitively the effects of the macroscopic viscosity, those involved in particle reorientations may not do so. To add more intrigue, for non-spherical molecules, rotational motions about specific axes appear decoupled from the macroscopic viscosity, while others retain such coupling.

Still within a hydrodynamic description, that is, an extension of thermodynamics that recognizes the dependence of extensive variables on spatial coordinates, we now see what happens when a particle diffuses, leaving a given volume element due to random microscopic encounters. Such a mass defect will generate a particle flux to recover the local equilibrium. The solution yields an expression for the self-correlation function for the density fluctuation caused by diffusion [4] which contains both algebraic $D_{\rm T}t^{-3/2}$ and $D_{\rm T}t^{-3}$ decay terms. This result reveals the complicated dynamics which a tagged particle experiences within a fluid as a result of its coupling with the density and momentum fields. A description of those processes involved in the decay of fluctuations such as those caused by a diffusing particle is known to require, for a single-component monoatomic liquid, a minimum set of three density components for the extensive variables such as the mass, momentum and energy densities. To specify a characteristic time scale for these processes which explicitly involves collisions with neighboring particles, recourse is made to the simplest case where an additional timescale $\tau_{\rm eff}$ is brought in by recourse to the Maxwell picture of a fluid element, and it is equated to the relaxation time for the viscosity. From here on, theory guides us on how to calculate the quantities accessible to experiment such as the double Fourier transform of the distinct density-density correlation function, that is the coherent $S(Q,\omega)$ dynamic structure factor measured with neutrons or X-rays.

Here we review some recent experiments covering several different aspects of liquid dynamics. Our aim is to illustrate, using whenever possible the same material, the multiplicity of timescales encompassed by different kinds of molecular motions, going from simple diffusive processes in low viscosity liquids to the description of the collective response of the fluid within the microscopic realm.

2. Experimental techniques

2.1. Neutron scattering

Contrary to other experimental probes, inelastic neutron scattering encompasses a wide range of energy (0.1μeV-1 eV) and momentum transfers ($10^{-2}-50$ Å^{-1}). In addition, the spin dependence of the neutron-nucleus cross sections allows us to study, in suitably chosen cases, both single-particle and collective dynamics in the same set of experiments. Put into different words, neutrons are capable of sampling particle motions having characteristic times shorter than ≈100 ns, which for neat liquids in their stable phases comprise both stochastic and finite-frequency processes.

Data reported here for molten K were measured using the full polarization analysis option of the IN14 cold triple axis neutron spectrometer located at the Institut Laue Langevin (ILL), Grenoble, France [5]. High-resolution quasielastic neutron spectra for molecular H_2, liquid HF and 1-propanol were measured using the IRIS [6] spectrometer at the ISIS pulsed neutron source at the Rutherford Appleton Laboratory, United Kingdom [7]. Higher-energy data concerning collective

excitations for molten K, *para*-H_2 and DF were measured using the MARI [8] chopper spectrometer at ISIS, and the IN8 thermal triple axis machine at the ILL.

2.2. Muon spectroscopy

These measurements are closely analogous to those of T_2 (Trasverse Field relaxation) in conventional nuclear magnetic or electron spin resonance techniques. They are known collectively as μSR (muon spin relaxation or rotation) – an acronym clearly contrived to resemble ESR (electron spin resonance). In fact, our μSR studies combine analogies with both ESR and NMR (nuclear magnetic resonance), since the implanted positive muons can access both paramagnetic and electronically diamagnetic states. These elementary particles mimic the chemical behavior of protons, either by picking up an electron to form muonium ($Mu = \mu^+e^-$) – the analogue of atomic hydrogen (we refer to this as the paramagnetic fraction) – or else by thermalizing into diamagnetic states. In alcohols, ROH, this latter species is undoubtedly the positive ion $ROHMu^+$, formed in the manner of direct protonation. The labelled molecule is neutral and diamagnetic, i.e., a closed-shell species, and in its intra-molecular motions should closely mimic the host molecule. Data reported here correspond to measurements carried out using the EMU and MUSR muon spectrometers located at the ISIS pulsed muon source. Some explicit examples of relaxation spectra for this material are shown in our previous communication [24].

For additional information on the technique the reader may browse through [9].

3. Monatomic liquids

One of the pending issues of the physics of simple alkali-metal liquids concerns the origin of the quasielastic part of the spectrum of density fluctuations $S_c(Q,\omega)$. Here we consider the case of molten K which, as most alkali metals, is regarded as the closest physical realization of a hard-sphere liquid. Previous results regarding the experimental determination of the full $S_c(Q,\omega)$ [10] have shown the inadequacy of the hydrodynamic approach, valid at low momentum transfers, and which predicts a central, relaxing thermodiffusive mode with a line width given up to second order in Q by $D_\lambda Q^2$, where D_λ stands for the thermal diffusion coefficient. Beyond the hydrodynamic realm, our knowledge of the low-frequency part of $S_c(Q,\omega)$ mostly relies on results from kinetic theory [11] which tells that close to Q_p, that is, where the static $S(Q)$ structure factor shows its maximum, spectral line widths may be approximated by [11],

$$\Delta\omega_c = \frac{2D_E Q^2}{S(Q)[1 - j_0(Q\sigma) + 2j_2(Q\sigma)]}\,, \tag{1}$$

where D_E stands for a hard-sphere diffusion coefficient as given by the Enskog prescription, σ characterizes the size of the fluid particles and j_x are spherical bessel functions of order x. Data given in [11] for liquified rare gases and molten rubidium show a reasonable agreement between line widths determined by experiment and equation (1), as also does more recent data on more complex liquids such as Ga, molecular D_2 or molten Ni [11,12]. Such results conform to the prediction of equation (1) provided that the value for D_E is set to that given by the mass-diffusion coefficient. As a result, the quasielastic part of $S_c(Q,\omega)$ is understood as a self-diffusion-like process of the liquid particles that enables the relaxation of density fluctuations.

In contrast, the $S_s(Q,\omega)$ spectra comprising the single-particle dynamics is known to follow, within the hydrodynamic realm, an exponential relaxation process, as dictated by Fick's Law with a decay constant given in terms of the self-diffusion coefficient D_s which in frequency space translates into a lorentzian line shape of width $D_s Q^2$ and peak height proportional to $1/D_s Q^2$. Beyond the hydrodynamic limit, usually located at momentum transfers of the order of 10^{-2} Å^{-1}, the behavior of $S_s(Q,\omega)$ is now understood quantitatively [13,14], mostly as a consequence of developments of kinetic theories of the mode-coupling family. These have provided us with predictive capabilities of accounting for the shape and characteristic parameters (i.e. wave vector dependence of its line width and amplitude) of the single-particle spectrum. The picture that emerges from these

theoretical approaches portrays motions within the kinetic regime, that is, for time-length scales comparable with inter-particle separations and microscopic times mediated by collective modes. For temperatures close to melting, coupling of particle diffusion to a longitudinal mode results in a retardation of diffusive motions if compared to the hydrodynamic prescription [14]. In contrast, diffusive dynamics at higher temperatures is thought to couple to transverse modes.

Some recent measurements of the quasielastic parts of both $S_{\rm c}(Q,\omega)$ (coherent) and $S_{\rm s}(Q,\omega)$ (self) have been performed by means of fully polarized neutron quasielastic scattering, in order to compare the characteristic times involved in both single-particle and collective-diffusion processes as well as the relationship between the Q dependence of their corresponding line widths $\Delta\omega_{\rm c}$ and $\Delta\omega_{\rm s}$. Although the ratio of coherent to incoherent neutron scattering for K is about 6.18, the coherent intensity, especially at low Q and low frequencies, is too weak to be separated by means of model fits to the spin-independent neutron double differential cross section. Such a separation can, however, be achieved by means of scattering experiments using polarized neutrons.

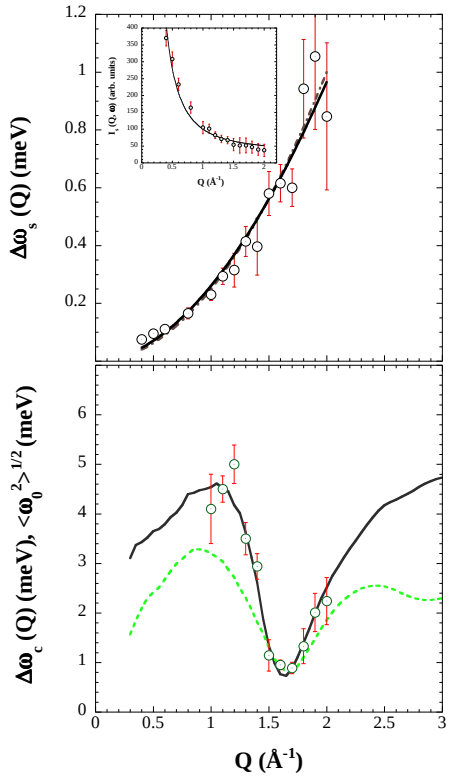

Figure 1. (Color online) The upper frame shows $\Delta\omega_{\rm s}(Q)$ (symbols) together with a fit to $D_{\rm eff}Q^m$. The dash-dot line depicts the best fit achieved using a quadratic, Fickian behavior. The inset displays the measured intensity $I_S(Q,\omega=0)$ (symbols) and the solid line displays a fit to $\propto 1/D_{\rm eff}Q^m$ prediction (see text). The lower frame shows $\Delta\omega_{\rm c}(Q)$ (symbols) together with a comparison to the prediction made from equation (1) using σ=4.7 Å and $D_{\rm eff}$= 0.24 meV Å^2 (solid line). The dashed line depicts the estimated wavevector dependence of the reduced second-frequency moment (see text).

Data shown in the upper frame of figure 1 displays the linewidths and amplitudes of a lorentzian signal fitted to $S_{\rm s}(Q,\omega)$. The best joint fit for both the linewidth and amplitude to power laws in $D_{\rm eff}Q^m$ and $[D_{\rm eff}Q^m]^{-1}$, respectively, yields a subquadratic Q dependence $\Delta\omega_{\rm s}(Q) = 2D_{\rm eff}Q^m$ with a value for the apparent diffusion coefficient $D_{\rm s}^{\rm eff} = 0.26$ (3) meV Å^m and an exponent $m = 1.87$ (28). A quadratic law yields a somewhat smaller value for the diffusion coefficient $D_{\rm s}^{\rm eff} = 0.24$ (9) meV Å^2 and a poorer fit. The value for the diffusion coefficient comes significantly short of the macroscopic value of 0.327 meV Å^2. Such retardation of diffusive processes at microscopic scales is usually attributed to a strong coupling with longitudinal collective modes [13,14]. Put into different words, under the present conditions mass diffusion only takes place after a relatively large lapse of time where liquid cages become incapable of maintaining collective oscillatory motions. Spectral peak intensities also follow such a sub-Fickian behavior and are well accounted for by introducing a further fitting parameter to serve as an overall normalization constant.

The reduction in value of the self-diffusion coefficient with respect to that obtained in the macroscopic limit serves to evaluate the importance of the coupling to collective and slowly varying dynamical modes. These ideas can be put into numbers by first evaluating the diffusion coefficient for a hard-sphere fluid $D_{\rm E}$ within the Enskog prescription in terms of the temperature, particle mass and packing fraction as [14],

$$\tilde{M}^{\rm MC}(\mathrm{i}\omega=0) = \frac{k_{\rm B}T/M}{D_{\rm s}^{\rm eff}}\left[1-\frac{D_{\rm s}^{\rm eff}}{D_{\rm E}}\right], \qquad (2)$$

and dividing it by the value for $D_{\rm s}^{\rm eff}$ given by the quadratic fit. Equation (2) yields the mode-coupling contribution to the Laplace trans-

form of the memory-function associated with the normalized particle velocity autocorrelation function $\langle v(t) \cdot v(0)\rangle / \langle v^2 \rangle$ at zero frequency. It yields a value of 11.2 ps^{-1} which comes to be about twice the value reported for molten Na at an equivalent temperature [14].

Data for the coherent line width $\Delta\omega_c(Q)$ also shown in figure 1 displays a narrow minimum at Q_p and its overall shape displays an oscillation along the curve giving the Q dependence of the incoherent linewidths. Within the region where equation (1) holds, that is about Q_p and somewhat beyond, the linewidth of the coherent component can be reproduced in terms of a single parameter which is set to the value of the experimentally determined self-diffusion coefficient, since a value for the particle diameter of about 4.7 Å was determined from the analysis of a previous inelastic experiment [10].

The picture that emerges from the data just commented on portrays an intimate relationship of the microscopic motions appearing in $S_c(Q,\omega)$ to those observable in the single-particle quantity $S_s(Q,\omega)$. Our data also show that diffusion-like processes either seen through the motions of a tagged particle in $S_s(Q,\omega)$ or given in terms of dynamic correlations between diffusing particles by $\Delta\omega_c(Q)$ take place within significantly different times scales. To illustrate such differences we plot in figure 2 the wave vector dependence of the inverse of the incoherent linewidth $\tau_{dif}(Q) = 2\pi/\Delta\omega_s$ as derived from the fits to the experimental values, the inverse of the coherent quasielastic linewidth $\tau_{str}(Q) = 2\pi/\Delta\omega_c$ as measured in the present set of experiments, and the relaxation time τ_{eff} associated to the propagation of longitudinal acoustic excitations, as studied in previous works [10]. Hence, a neat separation in timescales between the processes involving particle vibratory oscillations as sampled by τ_{eff} and mass transport phenomena explored through $\tau_{dif}(Q)$ and $\tau_{str}(Q)$ is inferred.

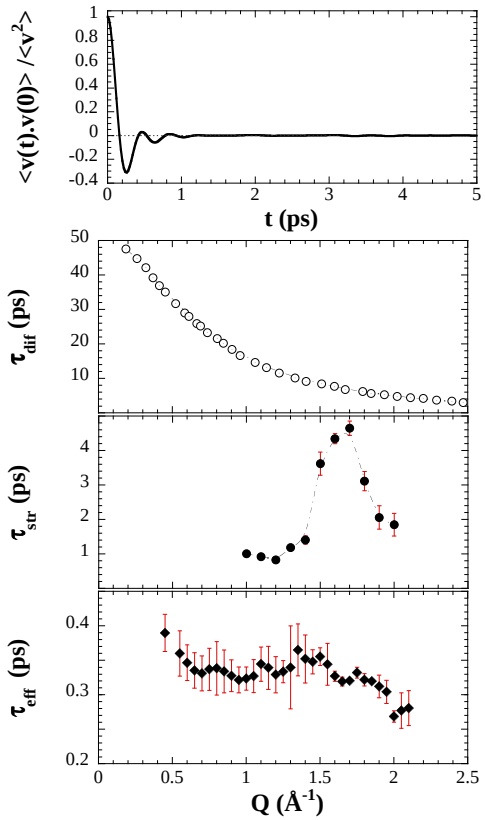

Figure 2. The upper frame displays the normalized particle VACF as calculated from the simulation results. Frames below depict the characteristic times associated with self-diffusion processes τ_{diff}, the inverse of the coherent quasielastic linewidth τ_{str} as calculated from the current set of experiments, and the relaxation time associated with the propagation of longitudinal acoustic excitations τ_{eff}, which was derived in previous studies [10].

The graphs drawn in figure 2 together with the plot showing the normalized velocity time correlation function (VACF) $\langle v(t) \cdot v(0)\rangle / \langle v^2 \rangle$ calculated from a simulation [10] show that microscopic vibratory motions take place at times shorter than some 0.5 ps where the VACF exhibits a strong oscillatory structure including a strong back-scattering (negative) region between 0.15 ps and 0.45 ps indicative of backflow effects. Such time range compares well to the average time between collisions $t_{coll} = 0.17$ ps estimated from the thermal velocity $v_{th} = 4.52$ Å ps^{-1} as well as from the mean free path given by $l = (\sqrt{(2)}\pi\sigma^2 n)^{-1} \approx 0.8$ Å . Relaxation phenomena sensed by quantities such as τ_{str} and τ_{dif} set in at times where all the oscillatory structure in the VACF has died away. Correlated particle diffusion, that is, the translational motions of particles within the microscopic liquid structures or cages sets in right after the complete decay of a density oscillation (sound mode). τ_{str} displays a strong momentum-transfer dependence with a narrow maximum at the peak of the

structure factor $S(Q)$ and therefore suggests that these phenomena are linked to "structural relaxation" effects. Notice, however, that long-range particle diffusion leading to liquid-flow effects takes place at significant longer times, as comparison of graphs for $\tau_{\rm diff}$ and $\tau_{\rm str}$ vividly exemplifies.

4. Molecular and complex liquids

Here we will briefly comment on two paradigmatic cases where the presence of multiple timescales involving diffusive and finite-frequency motions has been firmly established by experimental means.

4.1. Diatomics: Fully separated rotations and translations

The molecular hydrogens, H_2, D_2 and HD, constitute a particularly useful benchmark for the investigation of microscopic liquid dynamics. Their rather particular characteristics are best assessed by comparison of two measures of quantum behavior for translational and rotational motions, namely, $\lambda_{\rm T} = \hbar(M\epsilon\sigma)^{-1/2}$, usually known as the de Boer parameter and $\lambda_{\rm R} = (2B/\varepsilon_\phi)^{1/2}$ which is its rotational analogue. Here $\epsilon = 36.7$ K and σ =2.96 Å are the potential parameters for a Lennard-Jones potential, M stands for the molecular mass, $B = \hbar^2/2I$ is the rotational constant given in terms of the moment of inertia, and ε_ϕ sets an energy scale for the rotational motions. While $\lambda_{\rm T} = 0.274$, 0.224 and 0.193 provides a measure of quantum effects for translational motions and compares to 0.479 for He or 0.0355 for N_2, $\lambda_{\rm R} = 4.78$ for H_2 and 3.09 for D_2 provides a measure of the quantum nature of rotational motions and are to be compared to a meagre 0.46 for N_2.

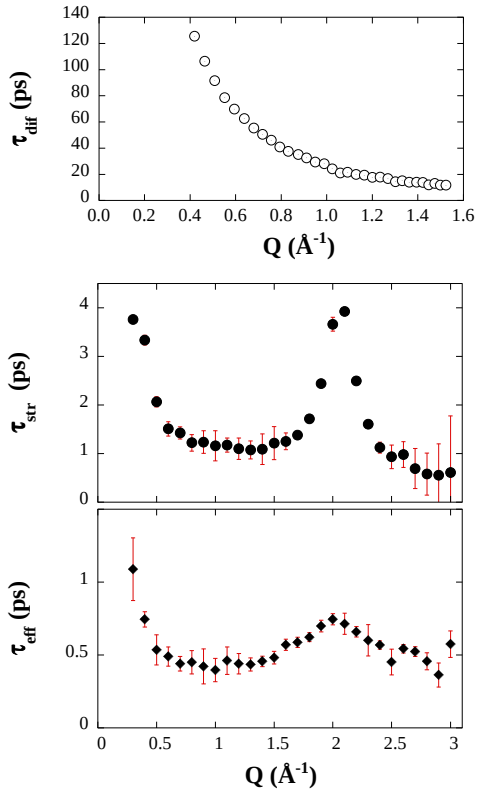

Figure 3. The upper frame displays the characteristic times associated with self-diffusion processes $\tau_{\rm dif}$ for molecular H_2, the inverse of the coherent quasielastic linewidth $\tau_{\rm str}$ as calculated from the current set of experiments and the time associated with the propagation of longitudinal acoustic excitations $\tau_{\rm eff}$, which was derived in previous studies [29].

The large value of the rotational constant for hydrogen $B = 85.25$ K (≈ 7.35 meV) [15] together with a consideration of the rotational spacing given by rigid-rotor energy eigenvalues $E_J = BJ(J+1)$ means that spectral transitions from the *para*$-H_2$ ground state to the first rotationally excited state will take place at ca. 15 meV, and therefore it is well separated from quasielastic and inelastic parts of the spectrum originating from centre-of-mass translations. A characteristic timescale for rotational motions is given in terms of the inverse of the rotational frequency and amounts to ca. 0.3 ps. Due to the quantum nature of such *para* $\longrightarrow$ *ortho*-H_2 transition (necessarily involving a nuclear-spin flip), spectral broadenings of this rotational transition are only caused by interactions with neighboring *ortho* molecules, and are estimated to be of the order of several tens of μeV. We note in passing that a separation between translations and internal rotations in H_2 is likely to break down when it is confined in strongly interacting substrates, as recently shown in neutron scattering studies of H_2 adsorbed in carbon nanohorns [26].

Under equilibrium (SVP) conditions, liquid hydrogen is primarily in its rotational ground state as *para*-$H_2(J = 0)$ and the lowest frequency motions correspond to diffusive mass transport. A recent experiment [26] has measured in detail such translational spectra for a 75:25 *ortho:para* H_2 mixture, which was chosen to isolate the single-particle spectrum since

para-H_2 is a mostly coherent scatterer of cold neutrons. Such measurements provide an experimental estimate of $\tau_{\rm dif}$ in much the same way as derived for molten K. Here, due to the large differences in neutron cross-sections between the lowerst-lying *ortho*- and *para*-H_2 species, our measurements provide direct access to self-diffusion of the *ortho* nuclear-spin isomer. The results are depicted in the upper frame of figure 3 and show that at low wave vectors, the characteristic times scales are above 100 ps. Also shown in figure 3 are data pertaining to the inverse of the coherent quasielastic linewidth $\tau_{\rm str}$ which, for reasons given earlier, we associate with structural relaxation effects. Such data were derived from coherent quasielastic scattering of *para*-H_2 in a different experiment. Remarkably, $\tau_{\rm str}$ displays a narrow maximum at wave vectors where $S(Q)$ shows its maximum.

The spectrum of finite-frequency excitations for a liquid of particles interacting via a spherically symmetric interaction potential such as *para*-H_2(J=0) only contains acoustic phonons [29]. Thus, characteristic times are to be compared with diffusive processes here defined as the inverse of the phonon linewidth, that is, an estimate of excitation lifetimes. The data plotted as $\tau_{\rm eff}$ in figure 3 are thus analogous to the same quantities derived for molten K and plotted in figure 2. They were derived from previous experimental works devoted to the spectrum of collective excitations [29].

A comparison between data shown in figure 2 and those in figure 3 reveals a substantial similitude in terms of the temporal scales involved in diffusion-like and propagating excitations. The similitude is most striking if allowance is made for the rather different systems involved, namely, a molten metal at $T = 370$ K and an insulating material at $T = 14$ K, the latter being characterized by strong quantum effects.

4.2. Diatomics: Experimental separation of timescales

Here we wish to illustrate the emergence of two additional timescales in the stochastic dynamics of molecular liquids. The first and the lowest in frequency of the two timescales arises from small particle reorientations about the molecular centre of mass taking place at an average zero frequency. Such motions, usually lumped together as rotational diffusion, are common to all molecular liquids and their spectra is not always easy to isolate from contributions to the total spectral intensity arising from translational and collective dynamics. The second timescale concerns collective dynamics at high-frequencies due to concerted, out-of-phase motions of neighboring molecules, which are reminiscent of optic-like excitations occurring in the parent crystals.

Our system of interest here is hydrogen fluoride (HF), which is known to have the strongest as well as the simplest hydrogen bond. These features make liquid HF a model system to which the behavior of more complex liquids such as water can be referred to.

Recent experiments [27] have provided accurate data for the low-frequency diffusional dynamics of this liquid. Data plotted in figure 4 correspond to the inverses of the translational and rotational contributions to the quasielastic spectrum. The large differences in characteristic timescales for either motion permitted a reliable separation of these two modes in the total dynamic structure factor, accessible via inelastic neutron scattering.

Two features worth remarking relate to the rather disparate timescales in which molecular translation and rotational diffusion take place, a difference of one-to-two orders of magnitude, and also, as pointed out in [27], the striking differences in the thermal activation characteristics of both sets of motions. While $\tau_{\rm dif}$ is seen to be coupled to the shear viscosity and follows a modified Stokes-Einstein law, $\tau_{\rm rot}$ is effectively decoupled from such a quantity and shows a very mild dependence with temperature. Put into different words, while translational diffusion displays features common to molten alkali-metals such as K or liquid H_2, rotational motions take place on a far more rapid timescale and are weakly hindered by the potential fields of neighboring molecules. In this context, it should be noted that HF displays the largest known rotational constant for a diatom (B $\sim$ 2.6 meV) after H_2 [15] as well as dynamic and kinematic viscosities in the liquid that are 4–5 times smaller than those of water at ambient temperature. Also, quantum delocalization of the proton has been shown to play an important role in describing the properties of liquid HF [16]. Even though this feature has been largely neglected in the past, it is now within the reach of ab-initio molecular dynamics methodologies.

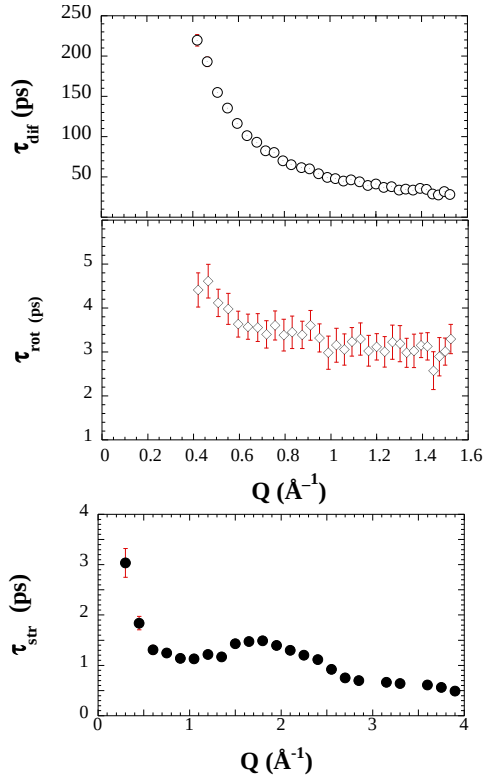

Figure 4. The upper frame displays the characteristic times associated with self-diffusion processes $\tau_{\rm dif}$ for hydrogen fluoride. The times associated with molecular reorientation processes are shown in the middle frame as $\tau_{\rm rot}$. The inverse of the coherent quasielastic linewidth $\tau_{\rm str}$ obtained from experiments using DF, a mostly coherent scatterer, is shown in the lower frame [30].

Recent experiments on liquid DF at $T = 205$ K, that is, a few degrees above melting did not reveal the presence of well-defined excitations at finite frequencies. The spectrum was describable in terms of a lorentzian component in addition to those attributable to the translational and rotational motions described above. The inverse of the spectral linewidths for such a lorentzian component is also shown in figure 4 as $\tau_{\rm str}$. With these data at hand, a comparison between figure 4 and figures 2 and 3 is in order, as both $\tau_{\rm diff}$ and $\tau_{\rm str}$ display common features in all three systems. The absolute timescales are not too dissimilar and appear within a relatively narrow interval. In fact, the main differences between such quantities for the three liquids are of a quantitative rather than a qualitative nature.

Interest in HF/DF also stems from reports from molecular dynamics simulations [17]. In these works, detailed analysis of the frequency spectrum for single-particle and collective motions shows the presence of well-defined finite-frequency features not accountable in terms of acoustic-like excitations. Recent neutron experiments employing relatively high incident energies [28] have confirmed the presence of such finite-frequency excitations in liquid DF at $T = 205$ K. These modes appear at around 28 meV and 80 meV, and have been assigned to an optic-like collective mode and to rapid molecular reorientational librations, respectively. Such relatively fast phenomena thus set the shortest times here considered to $\tau_{\rm vib} \sim 0.05 - 0.15$ ps.

5. Complex liquids: Dynamics under highly viscous regimes

Our last case to consider pertains the most extreme example of disparate timescales, namely, highly viscous liquids close to the liquid→glass transition temperature $T_{\rm g}$. The latter is currently viewed as a purely dynamical phenomenon characterized by metastable translational arrest, that is, a thermodynamic anomaly not related to any underlying phase transition [19]. Kinetic theories portray such a transition in terms of the onset of stochastic mass transport and reorientational motions signalling liquid-flow taking place beyond a characteristic temperature usually referred to as $T_{\rm c}$ located a few tens of Kelvin above the calorimetric glass-transition temperature $T_{\rm g}$. This theory constitutes the only predictive tool presently at our disposal which is capable of describing glassy phenomena in simple liquids [19], molecular liquids [22], and molecular crystals [23].

Due to the huge viscosities characteristic of a deeply supercooled liquid (SCL), one expects the above referred motions to be strongly coupled to others of vibrational nature that persist even within the glass-phase [20,21]. The presence of such strongly coupled motions poses a number of difficulties to isolate by experimental means phenomena related to the glass transition from others pertaining to the material characteristics which may exhibit distinct temperature dependences from that followed by translational mass-diffusion and may, therefore, hide any sign of criticality at $T_{\rm c}$, as has now been recognized [22].

Neutron quasielastic scattering on the molecular liquid 1-propanol (1Pr) within its normal and deeply supercooled liquid range [25] shows three different dynamic processes attributed to mass-diffusion with characteristic time $\tau_{\rm dif}$ and two molecular reorientational motions with times τ_{r1} and τ_{r2} attributable to reorientations along the principal molecular axis (methyl-group motions take place on much faster time scales). The temperature dependence of characteristic times for such motions is compared in figure 5 to that followed by the three main peaks (τ_α, secondary relaxation $\tau_{2^{\rm nd}}$ and τ_β) observed in the dielectric permittivity spectrum $\varepsilon(\omega)$.

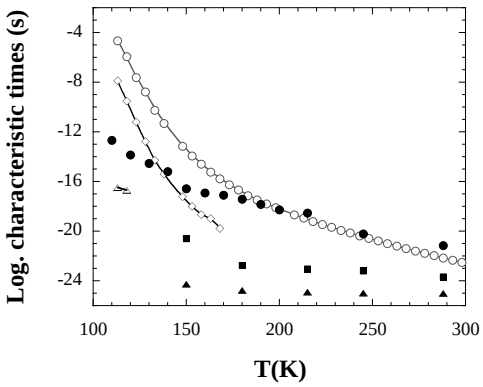

Figure 5. Dielectric relaxation times τ_α are shown by open circles, those characteristic of the high-frequency shoulder of $\varepsilon''(\omega)$ are shown by open lozenges and those for the β-type relaxation are shown by open triangles. Lines joining the data are guides to the eye. Neutron data are depicted by solid circles for $\tau_{\rm dif}$ and full squares and triangles for τ_{r1} and τ_{r2}, respectively.

Data shown in figure 5 span some ten orders of magnitude in dynamics. For temperatures well within the normal liquid range, that is, above $\sim$ 170 K (melting temperature $T_{\rm m}$ = 148 K), the dielectric τ_α and the neutron $\tau_{\rm dif}$ data merge with each other and follow similar temperature dependences. As the temperature is lowered towards melting and enters the SCL, dielectric and neutron data start to diverge. While τ_α exhibits a temperature dependence like that of the shear viscosity within the SCL range, all the three components of the neutron spectra show significantly milder temperature dependences. Furthermore, data for both τ_α and $\tau_{2^{\rm nd}}$ diverge as the temperature is lowered towards $T_{\rm g} = 98$ K, without showing any hint of criticality for $T_{\rm c} > T_{\rm g}$, whereas the neutron data follow a rather mild trend down to the lowest temperatures investigated.

Muon spin rotation (μSR) spectroscopy provides access to a frequency region intermediate between neutron and dielectric spectroscopy. μSR spectra yield relaxation or damping rates that are the simple inverse of the T_2 relaxation times: $\lambda_{\rm TF}(T) = T_2^{-1}(T)$. By heating from the glassy phase, these relaxation rates are expected to decrease with increasing temperature due to the onset of molecular motions: this is analogous to motional narrowing in NMR. The results are shown in figure 6 where one sees a mild decrease in relaxation rate accompanied by a small increase in signal amplitudes up to the calorimetric glass-transition temperatures. There are no distinct features at $T_{\rm g}$, but a strong drop in the relaxation rates, accompanied by a marked increase in signal amplitude, is seen at higher temperatures. Finally, a clear change of regime is attained for temperatures around 1.3 times $T_{\rm g}$, where the relaxation rates follow a smooth, approximately linear, dependence with increasing temperature.

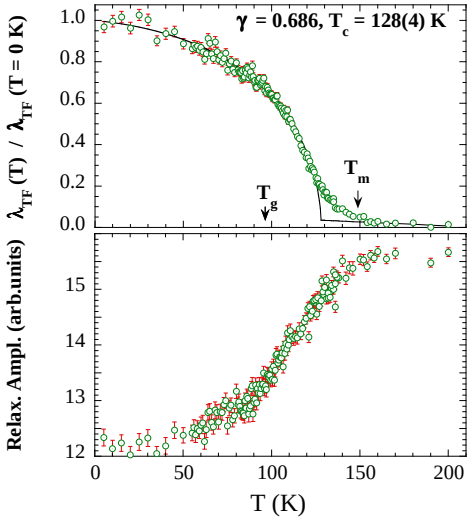

Figure 6. The upper frame shows the temperature dependence of the relaxation rate for 1PR under a transverse field of 20 G within its glass, deeply supercooled, and normal liquid ranges. The solid line shows the approximation described in the text. The inset shows the estimate for the critical temperature and γ factor (see text).

To model the data shown in figure 6 recourse is made to the predictions of Mode-

Coupling Theories (MCT) [19,22] concerning the Lamb-Mössbauer factor. On the grounds of such an analogy, we describe our data using a term proportional to $\sqrt{|T - T_c| / T_c}$, where T_c stands for a critical temperature, and the relaxation rate follows

$$\begin{aligned} \lambda(T) &= A\lambda_{\rm glass}(T)\sqrt{T_{\rm red}} + \zeta(T_{\rm red}), \qquad T \leqslant T_c\,, \\ \lambda(T) &= \zeta(T_{\rm red}), \qquad T > T_c \end{aligned} \tag{3}$$

with

$$T_{\rm red} = |T - T_c| / T_c, \qquad \zeta(T_{\rm red}) = \alpha_0 + \beta_0 T_{\rm red}. \tag{4}$$

The high temperature data is modelled by a mild, linear temperature dependence characterized by a slope easily calculated from the measured data once the value for T_c is set. Fitting the relaxation rates and leaving T_c and r as adjustable parameters yields a value of $T_c = 128(4)$ K, that is some 30 K above T_g, in agreement with theoretical predictions.

The result illustrates how the sought phenomena associated with the dynamic glass transition are best seen if the single-particle dynamics is explored within mesoscopic time scales, which are slower than 10^{-8} s but faster than some fraction of a millisecond. Motions within such limits are free from contributions from internal and deformational modes that considerably complicate the response of the SCL if explored using higher-frequency probes.

6. Concluding remarks

Our main aim in reporting on the four cases here considered was to illustrate the close interrelationships between the dynamics of a single-tagged molecule executing diffusion-like motions and cooperative rearrangements involving groups of particles within the liquid having an average zero frequency. From the data and arguments here given for $\tau_{\rm dif}$, we see that the Brownian diffusion regime is only achieved after some hundreds of picoseconds and that within such a lapse of time, many particle rearrangements with a characteristic time $\tau_{\rm str}$ will take place. In contrast, coherent motions of groups of particles with well-defined frequencies will take place within intervals of time spanning at most some tenths of a picosecond as clearly illustrated by data on $\tau_{\rm eff}$ and $\tau_{\rm vib}$.

The data here reported show that the characteristic times under consideration can only be related to relevant macroscopic transport coefficients such as that for the shear viscosity by means of SE or SED approaches under rather stringent conditions. Mass-diffusion motions as sampled by $\tau_{\rm dif}$ are certainly coupled to the viscosity within the normal liquid range but, as the data for our last case study show, diffusion within times far shorter than those characteristic of viscosity relaxation, may also take place. Even within the normal liquid range, recent data for HF have shown the emergence of fractional SE behavior [27], which marks a significant departure from Brownian dynamics approaches. Finally, the data shown here concerning rotational motions indicate that while SED behavior may constitute an apt prescription for the calculation of the rotational diffusion coefficient for a large object such a macromolecule or a colloidal particle immersed within a liquid composed of low-molecular-weight particles, its relevance to rationalize data concerning simple molecular liquids, should be considered as a first-order, rather approximate approach at best.

Finally, the current results point towards the need of further developments of theoretical tools capable of accommodating the current observations and thus bridging the gap between theory and experiment. In fact, theories on collective dynamics of liquids still lag well behind experimental observations and conversely, analysis of experimental data is many times carried out using expressions only valid within the hydrodynamic realm. Efforts carried out along the lines sketched by treatments based upon the Generalized Collective Modes [31] approach appear as a promising alternative and their further advancement should be pursued in order to develop a consistent framework useful in analyzing bare experimental data.

7. Acknowledgements

FFA gratefully acknowledges financial support from the UK Science and Technology Facilities Council.

References

1. Stokes G., Trans. Cambridge Phil.Soc., 1856, **9**, 5; Einstein A. Investigations on the Theory of Brownian Movement. Dover, New York, 1956.
2. Debye P. Polar Molecules. Dover, New York, 1945.
3. Gierer A., Wirtz K., Naturforsch Z., 1953, **8a**, 532; Hill N.E., Proc. Phys. Soc. London B, 1954, **67**, 149.
4. Keizer J. Statistical Thermodynamics of Nonequilibrium Processes. Springer, New York, 1987, p. 255.
5. http://www.ill.eu
6. Carlile C.J., Adams M.A., Physica B, 1992, **182**, 431.
7. http://www.isis.rl.ac.uk
8. Arai M., Taylor A.D., Bennington S.M., Bowden Z.A. In: Recent Developments in the Physics of Fluids, Howells W.S. & Soper A.K. eds, p. F291. Adam Hilger, Bristol, 1992.
9. http://www.isis.rl.ac.uk/muons/
10. a) Cabrillo C., Bermejo F.J., Alvarez M., Verkerk P., Maira-Vidal A., Bennington S.M., Martin D., Phys. Rev. Lett., 2002,**89**, 075508; b) Cabrillo C., Bermejo F.J., Alvarez M., Verkerk P., Maira-Vidal A., Bennington S.M., Martin D., J. Phys: Cond. Matter, 2004, **16**, S309.
11. Cohen E.G.D., Westerhuijs P., de Schepper I.M., Phys. Rev. Lett., 1987, **59**, 2872; For some recent tests see: Mondelli C., Gon'alez M.A., Albergamo F., Carbajo C., Torralvo C.M., Enciso E., Bermejo F.J., Fernandez-Perea R., Cabrillo C., Leon V., Saboungi M.L., Phys. Rev. B, 2006, **73**, 094206; Bermejo F.J., Bustinduy I., Levett S.J., Taylor J.W., Fernandez-Perea R., Cabrillo C., Phys. Rev. B, 2005, **72**, 104103.
12. Ruiz-Martin M.D., Jimenez-Ruiz M., Plazanet M., Bermejo F.J., Fernandez-Perea R., Cabrillo C., Phys. Rev. B, 2007, **75**, 224202.
13. Götze W., Zippelius A., Phys. Rev. A, 1976, **14**, 1842; Zippelius A., Götze W., Phys. Rev. A, 1978, **17**, 414; Wahnström G., Sjögren L., J. Phys. C: Solid State Phys., 1982, **15**, 410; Balucani U., Vallauri R., Phys. Rev. A, 1989, **40**, 2796.
14. Pilgrim W.C., Morkel C., J. Phys: Cond. Matter, 2006, **18**, R585; Morkel C., Pilgrim W.C., J. Non-Cryst. Solids, 2002, **312–314**, 128; Stangl A., Morkel C., Balucani U., Torcini A., J. Non-Cryst. Solids, 1996, **205 - 207**, 402;Morkel C., Gläser W., Phys. Rev. A, 1986, **33**, 3383.
15. Huber K.P., Herzberg G. Molecular Spectra and Molecular Structure IV. Constants of Diatomic Molecules. Van Nostrand, New York, 1979.
16. Raugei S., Klein M.L., J. Am. Chem. Soc., 2003, **125**, 8992.
17. Balucani U., Bertolini D., Stutman G., Tani A., Vallauri R., J. Chem. Phys., 1999, **111**, 4663; Bertolini D., Stutmann G., Tani A., Vallauri R., Phys. Rev. Lett., 1998, **81**, 2080; Garberoglio G., Vallauri R., Phys. Rev. Lett., 2000 **84**, 4878.
18. Cox S.F.J., Solid State NMR, 1998, **11**, 103.
19. Götze W., J. Phys: Condens.Matter, 1999, **11**, A1.
20. Caprion D., Matsui J., Schober H.R., Phys. Rev. Lett., 2000, **85**, 4293; Caprion D., Schober H.R., Phys. Rev. B, 2000, **62**, 3709; Fernández-Perea R., Bermejo F.J., Enciso E., Phys. Rev. B, 1996, **53**, 6215.
21. Cabrillo C., González M.A., Cuello G.J., Bermejo F.J., Saboungi M.L., Price D.L., Phys. Rev. B, 2004, **69**, 134202.
22. Schilling R., J. Phys.: Condens. Matter, 2000, **12**, 6311.
23. Ricker M., Schilling R., Phys. Rev. E, 2005, **72**, 011508.
24. Cabrillo C., Bermejo F.J., Cox S.F.J., Phys. Rev. B, 2003, **67**, 184201 (2003); Bermejo F.J., Bustinduy I., González M.A., Chong S.H. Cabrillo C., Cox S.F.J., Phys. Rev. B, 2004, **70**, 214202 (2004).
25. Bermejo F.J., Howells W.S., Jiménez-Ruiz M., González M.A., Price D.L., Saboungi M.L., Cabrillo C., Phys. Rev. B, 2004 **69**, 174201.
26. Fernandez-Alonso F., Bermejo F.J., Cabrillo C., Loufty R.O., Leon V., Saboungi M.L., Phys. Rev. Lett., 2007, **98**, 215503.
27. Fernandez-Alonso F., Bermejo F.J., McLain S.E., Turner J.F.C, Molaison J.J, Herwig K.W., Phys. Rev. Lett., 2007, **98**, 077801.
28. Bermejo F.J., Taylor J.W., McLain S.E., Bustinduy I., Turner J.F.C., Ruiz-Martin M.D., Cabrillo C., Fernandez-Perea R., Phys. Rev. Lett., 2006, **96**, 235501.
29. Bermejo F.J., Kinugawa K, Cabrillo C., Bennington S.M., Fak B., Fernandez-Diaz M.T., Verkerk P., Dawidowski J., Fernandez-Perea R., Phys. Rev. Lett., 2000, **84**, 5359.
30. Fernandez-Alonso F., McLain S.E., Taylor J.W., Bermejo F.J., Bustinduy I., Ruiz-Martin M.D., Turner J.F.C, J. Chem. Phys., 2007, **126**, 234509.
31. de Schepper I.M., Cohen E.G.D., Bruin C., van Rijs J.C., Mountfrooij W., de Graaf L.A., Phys.Rev. A, 1998, **38**, 271; Bryk T., Mryglod I., Condens.Matter Phys., 2004, **7**, 285.

Різні часові масштаби в мікроскопічній динаміці простих та складних рідин з досліджень по радіаційному розсіянню

Ф.Х.Бермехо[1], Ф.Фернандез-Алонсо[2,3], К.Кабрійо [1]

[1] Інститут структури матерії, Наукова Рада Досліджень та факультет науки та технології, Університет Паїс Васко, Більбао, Іспанія

[2] Лабораторія Резерфорд Аплтон, Чілтон, Великобританія

[3] Факультет фізики і астрономії, Лондонський університетський коледж, Лондон, Великобританія

Отримано 10 жовтня 2007 р.

Зроблено огляд експериментальних досліджень часових масштабів, що охоплюють колективну динаміку простих (металічних) та молекулярних рідин, на основі експериментів по розсіянню нейтронів та ротації спіна мюонів.

Ключові слова: *динаміка, рідини, стекла, розсіяння нейтронів, мюонна спектроскопія*

PACS: *61.25.Mv, 66.10.-x, 66.30.Fq, 65.20.+v*